RESEARCH ARTICLE OPEN ACCESS

Functional Profiling of Acetylcholine Receptor Antibodies Informs Therapeutic Outcome of FcRn Inhibitor Therapy in Myasthenia Gravis

Veronica Morcone,[1] Jacopo Morroni,[2] Giuseppe Valenzano,[1] Sofia Marini,[1] Silvia Falso,[1] Martina Marini,[1] Federico Habetswallner,[1] Giorgia Farì,[3] Cinzia Carrozza,[3] and Raffaele Iorio[1,2]

Correspondence
Prof. Iorio
raffaele.iorio@policlinicogemelli.it

Neurol Neuroimmunol Neuroinflamm 2026;13:e200616. doi:10.1212/NXI.0000000000200616

Abstract

Background and Objectives

Myasthenia gravis (MG) is an autoimmune disorder of the neuromuscular junction most commonly associated with acetylcholine receptor (AChR) antibodies (AChR-Abs), detected in up to 80% of patients. The emergence of targeted therapies, such as neonatal Fc receptor (FcRn) inhibitors, highlights the need for standardized functional assays capable of dissecting AChR-Ab pathogenic mechanisms. By selectively reducing circulating IgG through FcRn blockade, these agents differ fundamentally from conventional immunosuppressants, emphasizing the need to characterize antibody-mediated AChR dysfunction and complement activation as potential markers of therapeutic response. However, current functional assays often rely on transiently transfected or heterogeneous cell systems, limiting reproducibility and scalability. A stably transfected human cell line expressing physiologically clustered adult AChRs could fill this methodological gap and enable standardized, quantitative evaluation of antibody effector functions.

Methods

We generated a stable rhabdomyosarcoma (RD) cell line expressing clustered human adult AChRs (hAChR-RDcl) using the *PiggyBac* transposon system for genomic integration of AChR subunit genes. The hAChR-RDcl line was applied to functional cell-based assays using serum samples from 30 patients with AChR-MG before and after one treatment cycle with efgartigimod. Clinical efficacy was assessed by Quantitative Myasthenia Gravis (QMG) and MG Activities of Daily Living (MG-ADL) scores.

Results

The hAChR-RDcl cell line showed stable transcription and surface expression of adult AChR subunits, confirmed by RT-qPCR, α-bungarotoxin binding, and antibody-specific reactivity (mAb637 and patient serum samples). Baseline functional assays identified blocking antibodies in 15 of 30 (50%), internalizing antibodies in 20 of 30 (66.7%), and complement-activating antibodies in 14 of 30 (46.6%) samples. After efgartigimod treatment, all 3 antibody-mediated mechanisms were significantly reduced. Patients with persistent complement activity after treatment experienced more severe symptoms (higher QMG scores) compared with those showing other antibody-mediated pathogenetic mechanisms or complete suppression of antibody effector functions.

Discussion

The hAChR-RDcl cell line represents a reliable and scalable platform for standardized functional profiling of AChR-Abs. Functional characterization of AChR-Abs provides a translational approach to monitor therapeutic responses and elucidate the mechanisms underlying FcRn inhibitor efficacy in MG.

MORE ONLINE

Supplementary Material

[1]Department of Neuroscience, Università Cattolica del Sacro Cuore, Rome, Italy; [2]Neurology Unit, Fondazione Policlinico Universitario Agostino Gemelli IRCCS, Rome, Italy; and [3]Chemistry, Biochemistry and Molecular Biology Unit, Fondazione Policlinico Universitario Agostino Gemelli IRCCS, Rome, Italy.

The Article Processing Charge was funded by the authors.

Glossary

AChR = acetylcholine receptor; **AChR-Abs** = AChR autoantibodies; **CBA** = cell-based assay; **EFG** = efgartigimod; **FcRn** = Fc receptor; **gMG** = generalized MG; **HD** = healthy donor; **MFI** = mean fluorescence intensity; **MG** = myasthenia gravis; **MG-ADL** = MG Activities of Daily Living; **NMJ** = neuromuscular junction; **QMG** = Quantitative Myasthenia Gravis; **RD** = rhabdomyosarcoma.

Introduction

Myasthenia gravis (MG) is a chronic autoimmune disorder of the neuromuscular junction (NMJ) characterized by fluctuating weakness of voluntary muscles due to impaired neuromuscular transmission.[1] The disease is primarily mediated by autoantibodies targeting proteins expressed on the postsynaptic plasma membrane of the NMJ, most commonly the acetylcholine receptor (AChR), which are detected in approximately 80% of patients with MG.[2] AChR autoantibodies (AChR-Abs) impair synaptic transmission through multiple pathogenic mechanisms, including receptor blockade, AChR internalization, and activation of the complement cascade.[3,4]

Recent advances in MG therapy have led to the development of targeted immunotherapies such as inhibitors of the neonatal Fc receptor (FcRn), including efgartigimod (EFG),[5,6] which selectively lower circulating IgG by blocking FcRn-mediated IgG recycling.[7] The EFG efficacy on patients affected by generalized MG (gMG) has been demonstrated in multiple studies; however, a subset of patients exhibits limited response, reflecting the heterogeneity of MG pathogenesis and the diverse effector functions of AChR-Abs.[8,9] The relationship between FcRn inhibition and specific AChR-Ab pathogenic mechanisms—blockade, internalization, and complement activation—remains poorly defined.

Functional assays to study AChR-Abs often rely on transiently transfected or heterogeneous cell systems, limiting reproducibility and standardization.[4,10-12] To address this, we established a stable rhabdomyosarcoma (RD) cell line expressing physiologically clustered adult AChRs (hAChR-RDcl) as a reliable platform for mechanistic antibody profiling. Using this model, we examined pretreatment and post-treatment serum samples from patients with AChR-Ab–positive MG treated with EFG to evaluate changes in antibody-mediated functions and their correlation with clinical response. A schematic overview of the experimental design and workflow is illustrated in eFigure 1.

Methods

Study Population

We included patients with AChR-gMG, admitted at the outpatient clinic of Fondazione Policlinico Universitario Agostino Gemelli IRCCS between September 2023 and October 2025. Eligibility criteria comprised the following: (1) age ≥18 years; (2) a confirmed diagnosis of AChR-gMG according to current international guidelines; and (3) initiation of EFG in routine clinical practice, with completion of at least one full treatment cycle. In accordance with the Italian Medicines Agency prescribing criteria, EFG was administered to patients with a Myasthenia Gravis Activities of Daily Living (MG-ADL) score ≥5 and Myasthenia Gravis Foundation of America class ≥ IIb, who had shown inadequate response to at least one nonsteroidal immunosuppressive therapy. EFG was administered at a dose of 10 mg/kg as a 1-hour IV infusion, delivered in cycles of 4-weekly infusions. Serum samples were collected before the first and after the fourth infusion. Clinical response was evaluated using Quantitative Myasthenia Gravis (QMG) and MG-ADL scores, performed at the same time points. Clinical improvement was expressed as −ΔQMG and −ΔMG-ADL scores.

hAChR-RDcl Cell Line Generation

RD cell line (CCL-136; ATCC, Manassas, VA) was used as the parental line to generate a stable cell line expressing the human adult clustered AChR, designated hAChR-RDcl. Stable integration of AChR subunit genes was achieved using the *PiggyBac* transposon system.[13] RD cells were co-transfected with a plasmid encoding the PiggyBac transposase (pCM-pB) and 2 polycistronic vectors: one encoding CHRNA1 (AChR α1 subunit), CHRNB1 (β1 subunit), and RAPSN (rapsyn) and another encoding CHRND (δ subunit) and CHRNE (ε subunit). Transfections were performed with the JetPrime reagent (PolyPlus) according to the manufacturer's protocol, using a 1:2 DNA-to-reagent ratio and plasmid ratio of 2:2:1 (Vector1:Vector2:pCM-pB). Three days after transfection, antibiotic selection with puromycin and blasticidin (both 5 μg/mL) was applied for 21 days. To enhance receptor assembly and surface expression, cells were re-transfected with *piggyBac* vectors encoding CANX (calnexin) and pCM-pB (5:1 ratio) under identical conditions, followed by an additional 21 days of selection. Finally, cells were enriched for high AChR surface expression by cell sorting. Cells were stained with 1 μg/mL Alexa Fluor 488-conjugated α-bungarotoxin (AF488-α-BTX, Invitrogen, B13422) and 1 μg/mL DAPI (Sigma-Aldrich) for 30 minutes at 4°C in the dark. Live, α-BTX^{hi} cells were isolated using a BD FACSMelody Cell Sorter and expanded.

Real-Time PCR

Total RNA was extracted from hAChR-RDcl and parental RD cell lines using the Direct-zol RNA Microprep Kit (Zymo Research). RNA quality and concentration were assessed using a NanoDrop 1000 spectrophotometer (Thermo Fisher Scientific). Complementary DNA (cDNA) was synthesized

from total RNA using the LunaScript RT SuperMix Kit (New England Biolabs), according to the manufacturer's instructions. Quantitative real-time PCR (qRT-PCR) was performed on a QuantStudio1 system (Applied Biosystems, Thermo Fisher Scientific) using the Luna Universal qPCR Master Mix (New England Biolabs). Relative gene expression levels were calculated using the $2^{-\Delta\Delta CT}$ method and normalized to glyceraldehyde-3-phosphate dehydrogenase expression.

Cell Line Validation

Surface expression of AChR on hAChR-RDcl cells was validated by live cell-based assays (CBAs) and immunofluorescence staining. For CBAs, equal numbers of hAChR-RDcl and parental RD cells were mixed (1:1 ratio) and incubated for 30 minutes at 4°C with AChR-MG patient serum (1:100), or the AChR monoclonal antibody mAb637 (2 μg/mL). IgG binding was detected using Alexa Fluor 647–conjugated AffiniPure Goat Anti-Human IgG, Fcγ fragment–specific secondary antibody (1:500; Jackson ImmunoResearch), and DAPI (1 μg/mL) was used to exclude dead cells. In parallel, a CBA using AF488–α-BTX (1 μg/mL; Invitrogen, B13422) was performed by incubating hAChR-RDcl and parental RD cells separately under identical conditions. Samples were analyzed by flow cytometry on a CytoFLEX S instrument (Beckman Coulter).

For immunofluorescence staining, hAChR-RDcl and parental RD cells were seeded on chamber slides (Lab-Tek Chamber Slide System, #177402) and cultured for 48 hours and then fixed with 3% paraformaldehyde for 5 minutes. Cells were incubated with mAb637 (2 μg/mL) for 2 hours at room temperature, followed by an unconjugated goat anti-human IgG Fc secondary antibody (Invitrogen, #31125; 1:100) and donkey anti-goat IgG (H+L) Alexa Fluor 488 (Invitrogen, A11055; 1:200), each for 1 hour at room temperature. Nuclei were counterstained with DAPI (1 μg/mL). Methodological details on mAb637 production are provided in eMethod 1. Immunofluorescence images were acquired using a Nikon Eclipse Ti2 inverted microscope (Nikon Europe B.V., Amsterdam, The Netherlands) equipped with the CrestOptics X-Light V3 spinning disk system, the DeepSIM X-Light super-resolution add-on module (CrestOptics, Rome, Italy), the Celesta multimode multiline laser source (Lumencor, Beaverton, OR), and the Kinetix sCMOS camera (Teledyne Photometrics, Tucson, AZ). Further details on image acquisition are provided in eMethod 2.

AChR Antibody Testing by Radioimmunoprecipitation Assay

Serum AChR-Ab levels were determined using the *RiaRSR AChRAb* Kit (RSR Limited, Cardiff, United Kingdom) according to the manufacturer's protocol. Radiolabeled AChR (^{125}I–AChR) were incubated with 5 μL of patient serum for 17–21 hours at 2–8°C. Immune complexes formed between labeled receptors and serum Abs were precipitated using anti-human IgG. After the addition of 25 μL of precipitation enhancer, samples were centrifuged at 1,500×*g* for 20 minutes at 2–8°C and washed once, and the resulting precipitates were counted for 2 minutes in a gamma counter.

Measurement of AChR-Ab–Mediated Internalization Activity

To assess the ability of AChR-Ab to induce AChR internalization, hAChR-RDcl cells were incubated with heat-inactivated patient serum samples diluted 1:10 or mAb637 (2 μg/mL) for 1 hour at either 4°C or 37°C. Residual surface AChRs were detected under both conditions by staining with 1 μg/mL AF488-α-BTX as a probe for 30 minutes at 4°C in the dark. DAPI (1 μg/mL) was used to exclude dead cells. Samples were analyzed by flow cytometry on a CytoFLEX S instrument (Beckman Coulter). To quantify serum internalization capacity, we first compared AChR residual expression at 37°C and 4°C by calculating a scaled mean fluorescence intensity (MFI) (scaled MFI = MFI 37°C/MFI 4°C). Scaled MFI of healthy donor (HD) serum samples was then used as a normalization factor to correct for spontaneous AChR recycling. Serum internalization capacity was calculated as (scaled MFI)/ (HD scaled MFI). The internalization assay was also validated using a glycine-buffer stripping step (0.2 M, pH 2.5) to remove antibodies bound to the cell surface. Methodological details and corresponding results are presented in eMethod 3 and eFigure 2.

Assessment of AChR-Ab–Mediated Blocking Activity

The ability of AChR-Ab to block the binding of α-bungarotoxin (α-BTX), serving as a proxy for ACh to AChRs, was evaluated using the hAChR-RDcl cell line. hAChR-RDcl cells were first incubated with heat-inactivated patient serum samples diluted 1:10 or mAb637 (2 μg/mL) for 30 minutes at 4°C, followed by incubation with 1 μg/mL AF488-α-BTX for 30 minutes at 4°C in the dark. DAPI (1 μg/mL) was used to exclude dead cells. Samples were analyzed by flow cytometry on a CytoFLEX S. The blocking capacity of AChR-Abs was expressed as the fold change in MFI of AF488-α-BTX binding relative to HD controls.

Measurement of AChR-Ab–Mediated Complement Deposition

Complement activation capacity of AChR-Ab was evaluated using the hAChR-RDcl cell line. Cells were incubated with heat-inactivated patient serum diluted 1:20 or mAb637 (2 μg/mL) in the presence of normal human serum (NHS) depleted of complement component C8 (20% final volume; Sigma-Aldrich, C1538) for 1 hour at 37°C. Complement activation was assessed using a mouse anti-C3d primary antibody (Invitrogen, MA1-83965) for 30 minutes at 4°C, followed by a Cyanine5-conjugated goat anti-mouse IgG H&L secondary antibody (antibodies.com, A301660) for 30 minutes at 4°C in the dark. DAPI (1 μg/mL) was used to exclude dead cells. Samples were analyzed by flow cytometry on a CytoFLEX S. Complement activity was expressed as the fold change in median FI of Cyanine5-conjugated staining relative to HD controls. The assessment of IgM contribution to complement deposition is described in eMethod 4.

Statistical Analysis

Descriptive statistics were used to summarize all variables. Categorical data were expressed as counts and percentages while continuous data as means ± SD. Data normality was assessed using the Shapiro-Wilk test. For functional CBAs, positivity thresholds were defined as the mean scaled median FI ±3 × SD of healthy donors for complement activation and mean MFI–3×SD for blocking and internalization assays. Paired comparisons were analyzed using the ratio paired *t* test or Wilcoxon matched-pairs signed-rank test; unpaired comparisons used the Welch *t* test or Wilcoxon rank-sum test, as appropriate. For multiple-group comparisons, Brown-Forsythe and Welch ANOVA or Kruskal-Wallis tests were applied. Correlations were assessed using Pearson or Spearman coefficients (r or ρ) based on data distribution. Significance was set at $p < 0.05$. Incremental linear models were used to assess the association between complement activity and post-treatment QMG, adjusting for antibody titer changes. Logistic regression analyses were performed to examine the relationship between post-treatment antibody activity and clinical response (defined as a ≥5-point QMG reduction). Model performance and predictor selection were further evaluated using cross-validation and regularized regression approaches. Analyses were conducted in GraphPad Prism (v10.2.1) and R (v4.4.0) using the stats, logistf, glmnet, and pROC packages. Detailed model specifications are provided in eMethod 5.

Standard Protocol Approvals, Registrations, and Patient Consents

This study was approved by Ethics Committee of Università Cattolica del Sacro Cuore (protocol no. 130 ID #6717) and was conducted in accordance with the Declaration of Helsinki. All participants provided written informed consent prior to enrollment.

Data Availability

Anonymized data and hAChR-RDcl cell line will be shared at request by qualified investigators after the execution of appropriate material transfer agreements.

Results

Study Population

A total of 30 patients with AChR-gMG were enrolled, with a 20/30 male predominance (66.7%). Concomitant therapies (details in eTable 1) remained stable throughout the study period. A total of 60 paired serum samples were collected, immediately before the first infusion and at the fourth infusion of the treatment cycle. When a minimal reduction of ≥2 points in the MG-ADL score was applied, 24 patients (80%) were classified as MG-ADL responders; using a ≥3-point reduction threshold, 20 patients (66.7%) met the responder criteria. For the QMG score, a ≥3-point reduction defined 22 patients (73%) as responders, whereas a ≥ 5-point reduction classified 13 patients (43%) as QMG responders. Baseline demographics and clinical characteristics of the patient cohort and of the individual patients are summarized in Table 1 and eTable 1, respectively.

hAChR-RDcl Shows α, β, δ, and ε Subunit RNA Expression and Displays Surface Human Adult Clustered AChR

To validate expression of adult AChR subunit genes in hAChR-RDcl cells, qRT-PCR was performed to compare transcript levels of *CHRNA1, CHRNB1, CHRND, CHRNE, RAPSN*, and *CANX* between hAChR-RDcl and parental RD cells. All transfected transcripts were significantly upregulated in hAChR-RDcl cells, with *CHRND* and *CHRNE* exclusively expressed in this cell line (Figure 1A). Surface AChR expression was confirmed by CBAs through flow cytometry and immunofluorescence. AF488-α-BTX, AChR-MG patient serum, and mAb637 bound specifically to hAChR-RDcl cells, but not to parental RD cells (Figure 1, B–C). Furthermore, immunofluorescence staining with mAb637 revealed a punctate AChR distribution consistent with receptor clustering, which was absent in parental RD cells (Figure 1D).

Antibody-Mediated AChR Internalization, Blocking, and Complement Activation Decrease After EFG Therapy

We next used the hAChR-RDcl line to functionally characterize the diversity of AChR-Ab pathogenic mechanisms in a cohort of 30 patients with AChR-Abs–positive MG

Table 1 Demographic and Clinical Characteristics of MG Population Receiving Efgartigimod Therapy

Clinical features and demographics	Total (n = 30)
Female, n (%)	10 (33.33%)
Age at onset (y)	45.5 (16–88)
Age at efgartigimod initiation (y)	58.5 (23–89)
Disease duration (y)	8.5 (1–40)
Max MGFA classification	
Class I	0
Class II	5 (16.67%)
Class III	16 (53.33%)
Class IV	5 (16.67%)
Class V	4 (13.33%)
Thymoma	13 (43.33%)
Prednisone daily dose	20 (0–50)
MG treatment at baseline	
Oral corticosteroids	29 (96.67%)
Azathioprine	12 (40%)
Mycophenolate mofetil	7 (23.33%)
Cyclosporine	2 (6.67%)

Abbreviations: MG = myasthenia gravis; MGFA = Myasthenia Gravis Foundation of America.
Continuous and categorical variables are reported as median (range) and number (%).

Figure 1 Characterization of hAChR-RDcl Cell Line Expressing Human Adult AChR Subunits

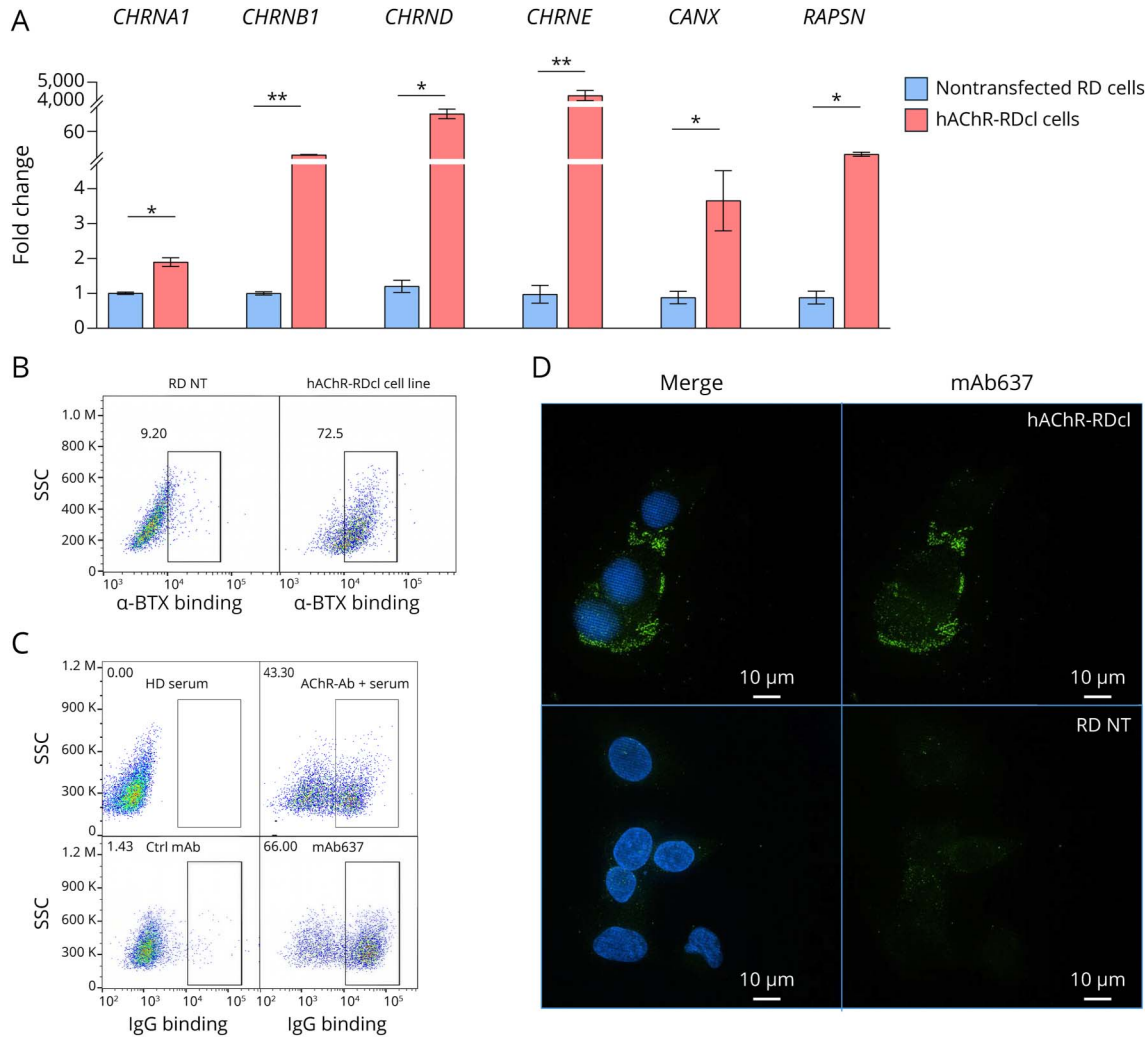

The successful integration and expression of *CHRNA1, CHRNB1, CHRND, CHRNE, RAPSN*, and *CANX* genes in hAChR-RDcl cells were confirmed by qRT-PCR and flow cytometry. (A) qRT-PCR analysis showing fold change in mRNA expression levels of *CHRNA1, CHRNB1, CHRND, CHRNE, RAPSN*, and *CANX* in hAChR-RDcl cells compared with parental nontransfected RD cells. All 4 subunits, *RAPSN* and *CANX* genes were significantly upregulated in hAChR-RDcl cells. (B) Representative dot plots showing α-BTX binding on RD NT and hAChR-RDcl cells. Strong α-BTX binding was observed in hAChR-RDcl but not RD NT cells, confirming surface expression of AChR. (C) CBA performed using a healthy donor serum and MG AChR-Ab$^+$ patient incubated with a mixed population of RD NT and hAChR-RDcl cells (upper). Representative CBAs showing IgG binding after incubation with a control monoclonal antibody (Ctrl mAb) or with the anti-AChR monoclonal antibody mAb637 incubated with a mixed population of RD NT and hAChR-RDcl cells (lower). Specific binding was observed only in hAChR-RDcl cells. (D) Representative immunofluorescence staining using mAb637 showing AChR clustering in hAChR-RDcl cells compared with parental RD cells. Data are shown as mean ± SEM. Statistical significance: **p* < 0.05, ***p* < 0.01, ****p* < 0.0001, *****p* < 0.00001.

receiving EFG treatment. At baseline, 20 of 30 patients exhibited detectable internalizing Abs (Figure 2A and eFigure 3A), 15 of 30 patients displayed blocking activity (Figure 2B and eFigure 3B), and 14 of 30 patients exhibited complement-activating Abs (Figure 2C and eFigure 3C). To determine the effect of EFG therapy on these mechanisms, paired analyses were performed both in the entire cohort and within subsets of patients who were positive at baseline for internalizing, blocking, or complement-activating Abs. Post-treatment serum samples demonstrated significantly reduced internalizing activity, with 10 of 20 patients achieving complete suppression of internalizing antibody activity and 10 patients retaining persistent, albeit reduced, internalizing capacity (Figure 2A and eFigure 4A). A similar decline was observed in blocking activity: 8 of 15 patients lost measurable blocking capacity after EFG therapy (Figure 2B and eFigure 4B). Conversely, only 3 of 14 patients lost detectable complement-activating Abs (Figure 2C and eFigure 4C). Detailed statistical results for all 3 functional assays are summarized in Table 2. The procedures used to define the optimal conditions for each assay are illustrated in eFigure 5. Because EFG does not reduce IgM levels and IgM can activate the complement cascade,[14] we examined whether AChR-IgM could contribute to persistent complement deposition after therapy. Among the 14 complement-positive patients at baseline, AChR-IgM was found before and after therapy in only one case (patient 19) (eFigure 6 and eMethod 4), who also showed ongoing complement deposition and limited clinical improvement.

Figure 2 Evaluation of AChR-Ab–Mediated Internalizing, Blocking, and Complement Activation Activity in Patients' Serum Samples Before and After EFG Therapy

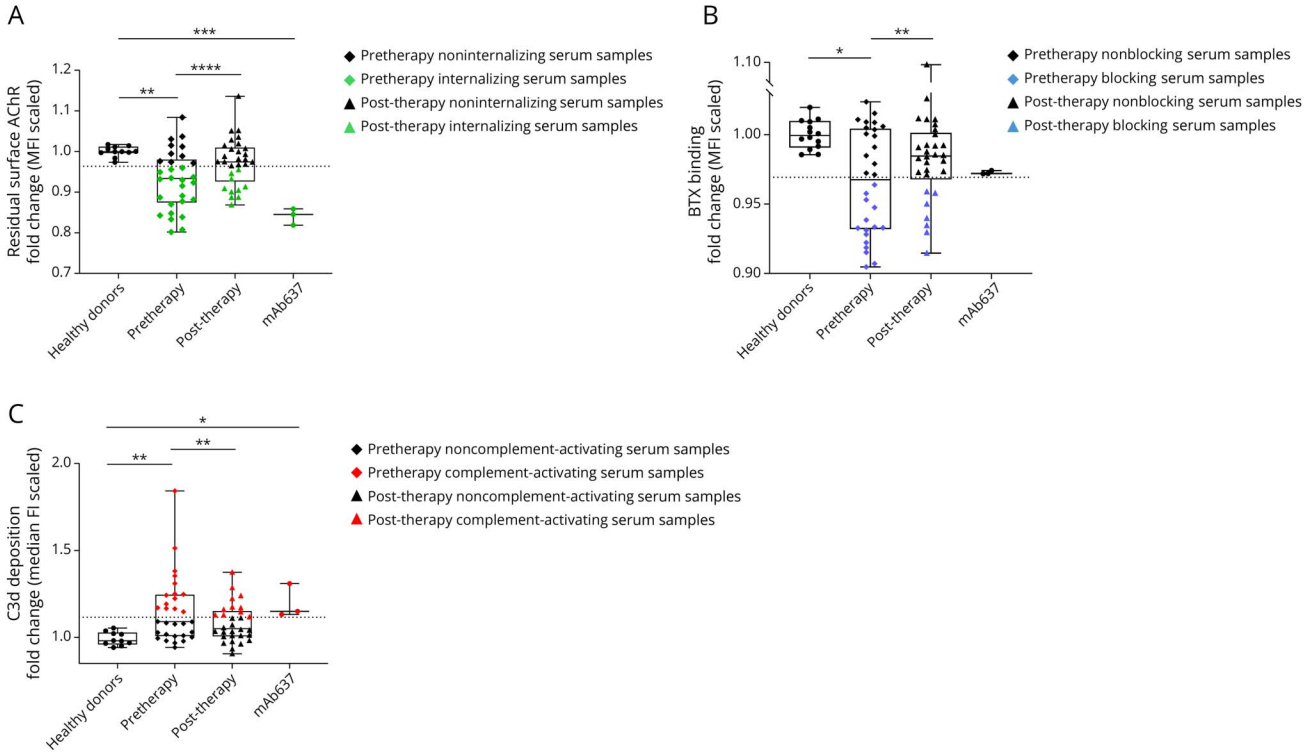

The capacity of serum samples from 30 patient AChR-Ab$^+$ serum samples to induce the internalization and blocking of AChR and activation of the complement cascade was assessed at baseline and after one treatment cycle with EFG. (A) Box plot showing baseline internalizing activity in patients' serum samples (N = 30) and after one cycle of EFG treatment, compared with healthy donors (N = 13) and mAb637. Internalizing Abs were detected in 20 of 30 patient samples (66.7%). After EFG treatment, 10 of 20 serum samples lost detectable internalizing activity, whereas the other half remained positive. The dotted line indicates the threshold for internalizing activity, defined as the mean MFI of healthy donors – 3X SD. (B) Box plot showing baseline blocking activity in patients' serum samples and after one cycle of EFG treatment (N = 30), compared with healthy donors (N = 14) and mAb637. Blocking Abs were detected in 15 of 30 patient samples (50%). After EFG treatment, 8 of 15 serum samples lost detectable blocking activity, whereas 7 of 15 remained positive. The dotted line indicates the threshold for blocking activity, defined as the mean MFI of healthy donors – 3X SD. (C) Box plot showing baseline complement activation ability in patients' serum samples and after one cycle of EFG treatment (N = 30) from patients scheduled to receive EFG treatment, compared with healthy donors (N = 10) and mAb637. Complement-activating Abs were detected in 14 of 30 patient samples (46.7%). After EFG treatment, 3 of 14 serum samples lost detectable complement deposition ability, whereas 11 of 14 remained positive. The dotted line indicates the threshold for complement activity, defined as the mean median FI of healthy donors +3 X SD. Box plots are shown as minimum to maximum values with the median. Statistical significance: *$p < 0.05$, **$p < 0.01$, ***$p < 0.0001$, ****$p < 0.00001$.

Table 2 Summary of Functional Assay Results for Internalization, Blocking, and Complement Activation Before and After Efgartigimod Treatment

	Internalization	Blocking	Complement activation
Baseline-positive patients, n (%)	20/30 (66.7%)	15/30 (50%)	14/30 (46.7%)
Baseline effect (mean ± SD)	11.2% ± 5.00[a]	7.1% ± 1.8[b]	30.4% ± 18.6[c]
Post-therapy effect (mean ± SD)	4.7% ± 5.4[a]	3.7% ± 2.4[b]	15.4% ± 10.7[c]
Mean absolute reduction (%)	6.48%	3.4%	14.7%
Post-therapy negative patients, n (%)	10/20 (50.0%)	8/15 (53.3%)	3/14 (21.4%)
Post-therapy positive patients, n (%)	10/20 (50.0%)	7/15 (46.6%)	11/14 (79,6%)

[a] Mean reduction of residual surface AChR assessed by AF488–α-BTX binding.
[b] Mean reduction of α-BTX binding due to competitive inhibition at the ACh binding site.
[c] Mean C3d deposition measured using C8-depleted serum.

Distribution of AChR Antibody–Mediated Pathogenic Mechanisms Before and After FcRn Inhibition Shows High Individual Variability

At baseline, serum samples from patients with AChR-MG displayed heterogeneous effector profiles, including internalization, blocking, complement deposition, or combinations thereof (Figure 3A). Three patients (patients 12, 18, and 21) showed no detectable pathogenic antibody activity at baseline. All 3 patients received multiple treatments before EFG (eTable 1), and functional assays for patient 21 were performed before/after the third cycle of EFG, which was administered for a mild worsening of MG symptoms. Notably, blocking value of patient 12 and complement activation value of patient 21 were close to the respective assay cutoffs. After EFG treatment, functional antibody activity was variably reduced across patients. While internalization and blocking activity were frequently diminished or lost, complement deposition persisted in a subset of patients (Figure 3B).

Of interest, comparative analysis of patients stratified by residual pathogenic profile—no detectable mechanisms (baseline negative plus post-treatment negative) (N = 12), persistent complement activation (N = 11), and other residual mechanisms without complement (N = 7)—revealed that the complement-positive group exhibited the highest post-treatment QMG scores compared with both groups (Figure 3C, eFigure 7). Accordingly, when patients were stratified according to clinical outcome (QMG ≥11 vs < 11; MG-ADL ≥2 vs < 2), post-treatment complement activation was significantly higher in patients with worse clinical status (Figure 3D).

Complement Deposition but Not AChR Antibody Titers Correlates With Clinical Outcome and Predicts Lower Clinical Improvement

Consistent with FcRn inhibition, AChR antibody titers were significantly reduced after EFG treatment (Figure 4A). However, neither post-treatment (Figure 4B) nor baseline antibody titers correlate with disease severity as assessed by QMG. Likewise, individual changes in antibody titers did not correlate with clinical improvement (eFigure 8).

Linear regression analysis revealed no association between individual changes in anti-AChR titers ($\Delta log10\ titers$) and changes in complement deposition ($\Delta C3d$) after EFG

Figure 3 Persistent Complement Activation Detected by Functional AChR Assays Correlates With Disease Severity

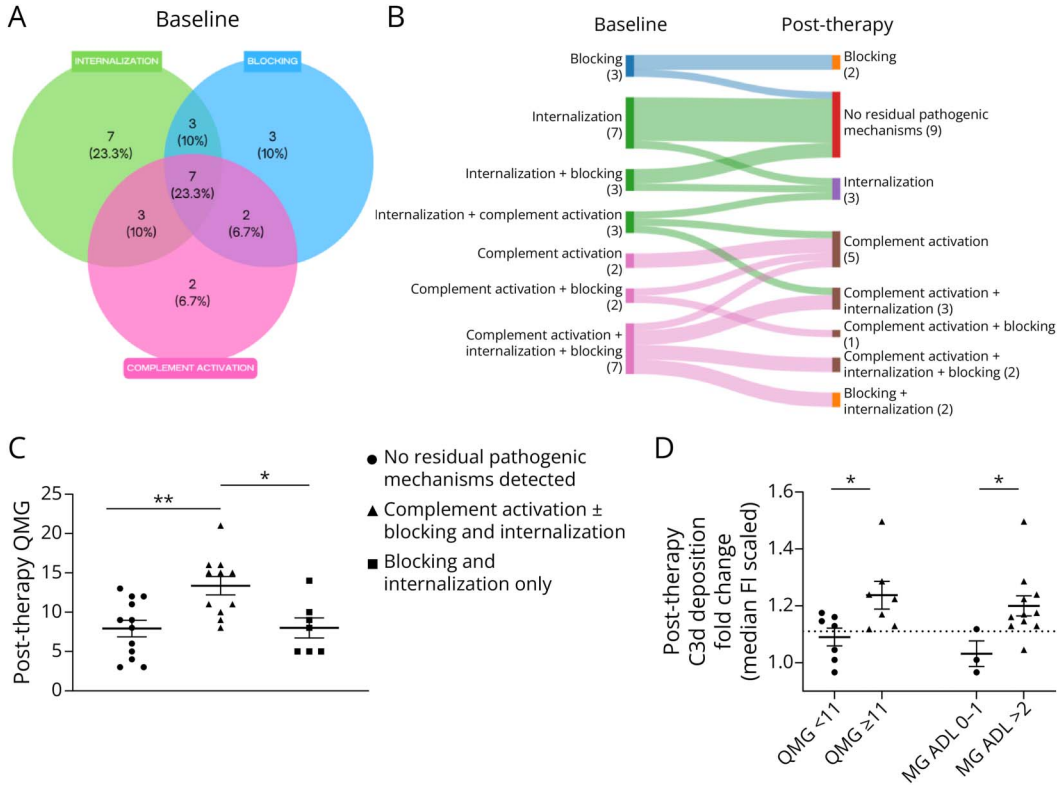

(A) Venn diagram and (B) Sankey plot depicting the distribution and evolution of AChR-Ab pathogenic mechanisms (internalization, blocking, and complement activation) before and after EFG therapy. Baseline serum samples displayed heterogeneous and overlapping pathogenic activities, while therapy induced a redistribution of these mechanisms with partial or complete functional suppression in a subset of patients. (C) Scatter dot plot comparing post-therapy QMG scores among patients stratified by residual pathogenic profiles: no detectable residual mechanisms, complement activation ± other mechanisms, and other noncomplement mechanisms. (D) Scatter dot plot showing post-therapy C3d deposition in patients stratified by clinical severity. Patients with higher QMG and MG-ADL scores (QMG ≥11 or MG-ADL >2) exhibited significantly greater post-therapy complement activation compared with patients with milder symptoms (QMG <11 or MG-ADL = 0–1). Statistical significance: *p < 0.05, **p < 0.01, ***p < 0.0001, ****p < 0.00001.

Figure 4 Complement Activation After Therapy—but Not AChR Antibody Titers—Correlates With Clinical Outcome and Predicts Limited Clinical Improvement

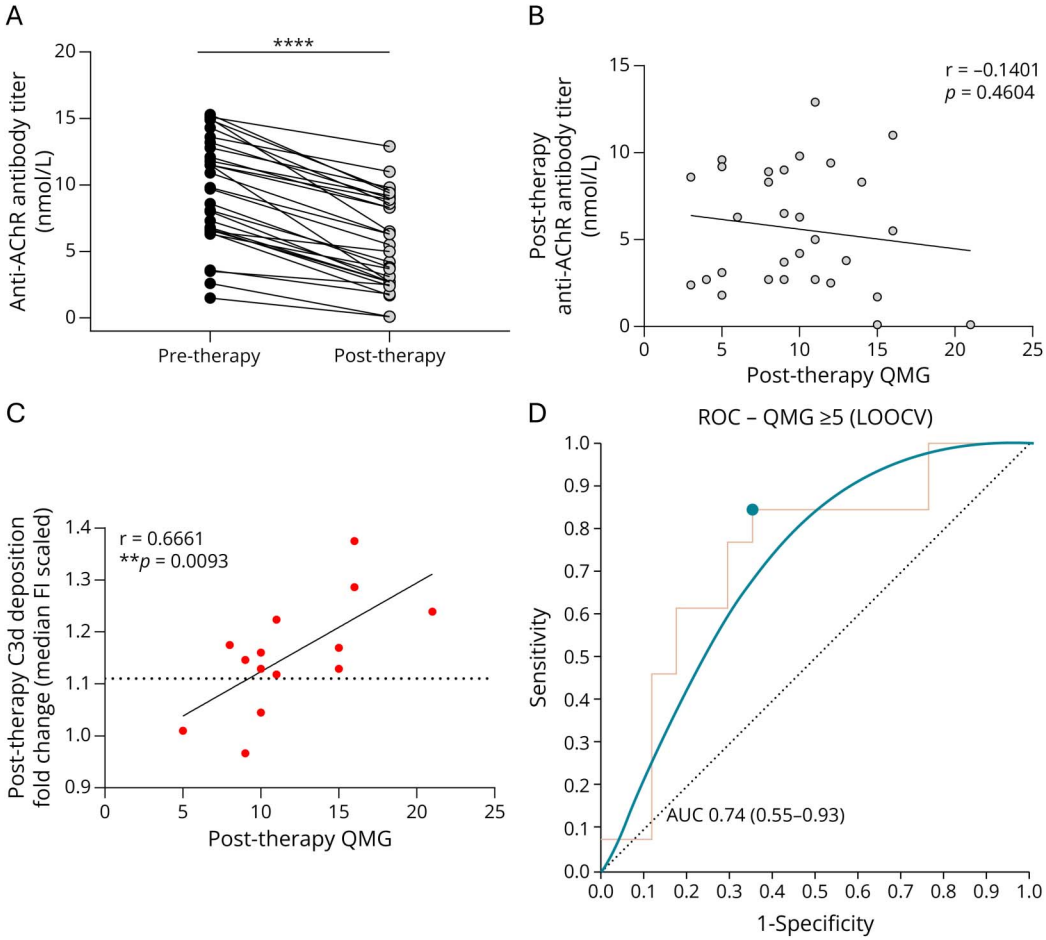

(A) Paired scatter dot plot showing anti-AChR antibody concentrations measured by radioimmunoprecipitation assay (RIPA) at the baseline before and after EFG treatment. A significant reduction in AChR-Ab levels was observed after treatment. (B) Linear correlation analysis showing no significant association between post-therapy anti-AChR antibody titers and MG severity (post-therapy QMG). (C) Linear correlation analyses showing significant associations between post-therapy C3d deposition and post-therapy QMG scores, indicating that complement activation detected by the hAChR-RDcl assay reflects clinical disease severity. (D) Model performance for QMG ≥5 response. Leave-one-out cross-validation (LOOCV) yielded an area under the curve of 0.74 (95% CI 0.55–0.93), indicating fair discrimination. The optimal Youden threshold (0.31) provided a sensitivity of 0.85 and specificity of 0.65. Statistical significance: *p < 0.05, **p < 0.01, ***p < 0.0001, ****p < 0.00001.

therapy (eFigure 9 and eMethod 5). By contrast, complement activation assessed by C3d deposition showed a positive association with disease severity. In particular, post-treatment C3d levels correlated with post-treatment QMG scores (Figure 4C, eFigure 10). Notably, when considering all 30 patients in our cohort, both pretherapy and post-therapy C3d levels exhibited a significant positive correlation with post-therapy QMG scores (eFigure 11 and eMethod 5).

Consistently, in incremental linear models examining the association with post-treatment QMG, the inclusion of post-therapy C3d deposition levels provided a significant improvement beyond Δtiter alone (p = 0.02 vs 0.008 and R^2 = 0.1481 vs 0.3262 for Δtiter alone and Δtiter + complement, respectively), thus indicating that complement activation adds clinically relevant information not captured by changes in antibody levels. Conversely, the inclusion of blocking and internalization values did not significantly improve the model fit (Table 3 and eMethod 5).

In logistic regression analyses, post-treatment complement activity was the only significant predictor of clinical response. Patients with complement activation above the post-treatment cutoff had markedly lower odds of achieving a ≥5-point QMG improvement (Firth OR = 0.11, 95% CI 0.007–0.80, p = 0.028) (eFigure 12). While the baseline QMG score was independently associated with achieving a ≥5-point reduction (Firth OR = 1.45, 95% CI 1.13–2.19, p = 0.001), internalization and blocking activity were not associated with clinical improvement.

Model performance assessed by leave-one-out cross-validation demonstrated good discrimination (area under the curve [AUC] = 0.74, 95% CI 0.55–0.93), with an optimal

Table 3 Incremental Linear Regression Modeling Shows That Post-Therapy Complement Activity, but Not Changes in Individual Antibody Titers, Correlates With Clinical Outcome

Model	Predictors (QMG_post ~)	Model pval (adj)	R^2 (adj)	ΔR2 vs m1	Partial R^2 (c3d/titer)	ANOVA vs m1
m1	Δlog10 titer	0.0204	0.1481	NA	NA	NA
m2	Δlog10 titer + c3d_post	0.0018	0.3262	0.1951	0.2373/0.1611	p = 0.0074
m3	Δlog10 titer + c3d_post + blocking_post + intern_post	0.0108	0.2996	0.0235	0.2003/0.1101	p = 0.6209
m4	Δlog10 titer + c3d_pre	0.0003	0.4070	0.2703	0.2944/0.1933	p = 0.0011

Abbreviations: Δlog10 titer = individual variation in anti-AChR antibody titers considering baseline and the end of the fourth EFG cycle; blocking_post = levels of MG serum-induced AChR blocking, expressed as fold-change compared with HC serum after EFG therapy; c3d_post = levels of MG serum-induced c3d deposition, expressed as fold-change compared with HC serum after EFG therapy; intern_post = levels of MG serum–induced AChR internalization, expressed as fold-change compared with HC serum after EFG therapy; QMG_post: QMG values after EFG therapy.

Youden threshold of 0.31 (sensitivity = 0.85, specificity = 0.65). In the LASSO analysis, complement activity after treatment was consistently retained as the strongest negative predictor (β = −1.15, OR = 0.32). The baseline QMG score was further selected (β = 0.24, OR = 1.28), reinforcing its contribution to treatment response (Figure 4D).

Discussion

In this study, we developed a stable RD cell line expressing the human adult clustered AChR (hAChR-RDcl) and used it to functionally profile the AChR-Ab repertoire in patients with MG treated with the FcRn inhibitor EFG. The use of a clustered AChR cell platform enabled the simultaneous assessment of antibody-mediated pathogenic mechanisms in patient serum samples and the investigation of their association with clinical response to FcRn treatment. After one treatment cycle, patients demonstrated clinically meaningful improvement, with significant reductions in both MG-ADL and QMG scores, consistent with response rates reported in previous studies of patients inadequately controlled by standard therapy.[15,16]

Current functional assays for AChR-Abs largely rely on transient transfection systems and multiple cell lines,[4,10-12,14] often resulting in variability, limited reproducibility, and low scalability due to batch-to-batch effects. Establishing a cell line that stably expresses human adult clustered AChRs overcomes these limitations by providing consistent receptor expression, minimizing experimental variability, and simplifying assay standardization. Moreover, the hAChR-RDcl cell line reproduces the native organization of adult clustered AChRs, providing a physiologically relevant platform for functional studies.

Using this platform, we assessed AChR-Ab–mediated pathogenetic mechanisms before and after EFG therapy. The frequency of internalizing Abs was consistent with previous observations.[11] As reported, AChR clustering limits antibody-mediated receptor internalization,[17] and accordingly, the magnitude of internalization detected in our system was lower than that described in nonclustered models.[11] EFG significantly reduced internalizing activity; however, neither baseline internalization nor its reduction correlated with clinical improvement, indicating that internalizing Abs are not the dominant determinant of short-term response to FcRn inhibition.

The percentage of detected blocking Abs falls within the range of previously reported frequencies.[18-21] It is worth noting that assays using fetal or unclustered AChRs may overestimate blocking activity[22] while our clustered receptor system may yield lower frequencies compared with unclustered systems. Blocking activity did not show an independent association with clinical improvement, consistent with evidence that blocking Abs represent one component of a heterogeneous pathogenic repertoire variably contributing to neuromuscular transmission failure.[22] Nevertheless, serum-based assays may underestimate the contribution of pathogenic antibodies acting specifically at the NMJ.

Complement-activating Abs were detected at a lower frequency than previously reported.[10,11] This difference likely reflects both cohort and methodological factors. Our patients were not treatment-naïve because EFG is indicated for patients with AChR-MG demonstrating inadequate clinical response to corticosteroids and at least one nonsteroidal immunosuppressive agent, and prior or ongoing immunotherapy may attenuate complement-mediated activity at the time of sampling. In addition, studies reporting higher frequencies often used HEK293T triple knock-out cells lacking complement regulators (CD46, CD55, CD59), thereby maximizing complement deposition.[10,11] By contrast, the hAChR-RDcl cell line retains physiologic expression of complement regulators, which can limit activation and may partly explain the lower rate observed in our cohort.[23-26] Furthermore, complement activation and other Ab-mediated mechanisms can fluctuate substantially over time within individual patients,[11] suggesting that single time-point measurements may underestimate their true prevalence.

After EFG therapy, complement-activating activity decreased significantly, although only 3 patients achieved complete

suppression. This persistence may reflect the strong complement-fixing capacity of anti-AChR IgG1 and IgG3 Abs, meaning that even low-level residual activation may sustain NMJ injury.[27,28] In addition, anti-AChR IgM may contribute to persistent complement activation in a minority of patients because EFG does not affect circulating IgM.

Indeed, residual complement activity correlated with higher post-treatment QMG scores and reduced likelihood of clinical response. Conversely, patients without detectable pathogenic mechanisms after therapy showed milder disease, indicating that results from the hAChR-RDcl assays correlates with clinical state.

No pathogenic activity was detected at baseline in 3 patients, 2 of whom showed borderline values, which may reflect antibody activity below detection thresholds or dynamic fluctuations in antibody pathogenicity not fully captured by the assays.

These findings reinforce complement-mediated injury as a dominant driver of NMJ dysfunction in AChR-MG. Consistent with this, changes in total AChR-Ab titers did not correlate with outcome, whereas residual complement activity after therapy correlated with disease severity. Moreover, the association between baseline complement activation and post-treatment QMG suggests that complement activity measured prior to therapy reflects biologically relevant disease features that persist after treatment.

Although this study focused on 3 well-established AChR-Ab–mediated mechanisms, additional Fc-dependent effector pathways, including antibody-dependent cellular cytotoxicity and phagocytosis, may also contribute to disease pathogenesis. Future studies incorporating Fcγ receptor–dependent assays and subclass-resolved analyses will be required to clarify the role of these mechanisms.

Our study has limitations. The sample size was relatively small and derived from a single center, and patients were heterogeneously treated at baseline, which may limit generalizability. Furthermore, although the hAChR-RDcl model closely approximates the adult NMJ environment, in vitro systems cannot fully recapitulate its complex synaptic architecture. Another limitation is the absence of control antibodies directed against unrelated antigens; however, the functional assays used are specific for AChR-dependent mechanisms and cannot be readily applied to other antigen systems.

Despite these limitations, the hAChR-RDcl platform provides a reliable and physiologically relevant system for standardized functional characterization of AChR-Abs. Functional profiling captures clinically relevant pathogenic activity that is not reflected by antibody titers alone.[29] Longitudinal functional testing could also support personalized treatment scheduling, allowing therapy to be administered based on pathogenic activity rather than fixed intervals. Monitoring for re-emergence of pathogenic Abs may facilitate early detection of relapses and inform timely therapeutic adjustments. Moreover, functional profiling of individual pathogenetic mechanisms could guide treatment selection (e.g., FcRn inhibition vs complement inhibition). Although exploratory, these results suggest that functional antibody profiling may represent a complementary biomarker to monitor pathogenic antibody activity and potentially inform disease prognosis over time. Future longitudinal studies across multiple treatment cycles are warranted to define the kinetics, durability, and prognostic value of functional antibody signatures in the evolving therapeutic landscape of MG.

Acknowledgment

The authors thank Prof. Alessandra Battaglia and Dr. Chiara Cimmino from flow cytometry facility in Fondazione Policlinico A. Gemelli for providing their expertise and criticism. The authors also thank CrestOptics S.p.A. (Rome, Italy) for providing their access to their super-resolution microscopy setup and for their technical expertise.

Author Contributions

V. Morcone: drafting/revision of the manuscript for content, including medical writing for content; major role in the acquisition of data; analysis or interpretation of data. J. Morroni: drafting/revision of the manuscript for content, including medical writing for content; study concept or design; analysis or interpretation of data. G. Valenzano: drafting/revision of the manuscript for content, including medical writing for content; major role in the acquisition of data. S. Marini: drafting/revision of the manuscript for content, including medical writing for content. S. Falso: drafting/revision of the manuscript for content, including medical writing for content. M. Marini: drafting/revision of the manuscript for content, including medical writing for content. F. Habetswallner: drafting/revision of the manuscript for content, including medical writing for content. G. Farì: drafting/revision of the manuscript for content, including medical writing for content; analysis or interpretation of data. C. Carrozza: drafting/revision of the manuscript for content, including medical writing for content; analysis or interpretation of data. R. Iorio: drafting/revision of the manuscript for content, including medical writing for content; study concept or design; analysis or interpretation of data.

Study Funding

The authors report no targeted funding.

Disclosure

S. Marini has received speaker honoraria from Alexion and UCB. S. Falso has received speaker honoraria from Alexion, Argenx, and UCB. R. Iorio has received consultancy fees and speaker honoraria from Alexion, Argenx, UCB, and Dianthus Therapeutics. The remaining authors have no conflicts of interest. Go to Neurology.org/NN for full disclosures.

Publication History

Received by *Neurology® Neuroimmunology & Neuroinflammation* November 10, 2025. Accepted in final form April 13, 2026. Submitted and externally peer reviewed. The handling editor was Associate Editor Marinos C. Dalakas, MD, FAAN.

References

1. Gilhus NE, Tzartos S, Evoli A, Palace J, Burns TM, Verschuuren JJGM. Myasthenia gravis. *Nat Rev Dis Primers*. 2019;5(1):30. doi:10.1038/S41572-019-0079-Y
2. Kaminski HJ, Sikorski P, Coronel SI, Kusner LL. Myasthenia gravis: the future is here. *J Clin Invest*. 2024;134(12):e179742. doi:10.1172/JCI179742
3. Rose N, Holdermann S, Callegari I, et al. Receptor clustering and pathogenic complement activation in myasthenia gravis depend on synergy between antibodies with multiple subunit specificities. *Acta Neuropathol*. 2022;144(5):1005-1025. doi:10.1007/S00401-022-02493-6
4. Pham MC, Masi G, Patzina R, et al. Individual myasthenia gravis autoantibody clones can efficiently mediate multiple mechanisms of pathology. *Acta Neuropathol*. 2023;146(2):319-336. doi:10.1007/S00401-023-02603-Y
5. Yang Y, Shen Z, Shi F, Wang F, Wen N. Efgartigimod as a novel FcRn inhibitor for autoimmune disease. *Neurol Sci*. 2024;45(9):4229-4241. doi:10.1007/S10072-024-07460-5
6. Iorio R. Myasthenia gravis: the changing treatment landscape in the era of molecular therapies. *Nat Rev Neurol*. 2024;20(2):84-98. doi:10.1038/S41582-023-00916-W
7. Ulrichts P, Guglietta A, Dreier T, et al. Neonatal Fc receptor antagonist efgartigimod safely and sustainably reduces IgGs in humans. *J Clin Invest*. 2018;128(10):4372-4386. doi:10.1172/JCI97911
8. Heo YA. Efgartigimod: first approval. *Drugs*. 2022;82(3):341-348. doi:10.1007/S40265-022-01678-3
9. Howard JF, Bril V, Vu T, et al. Safety, efficacy, and tolerability of efgartigimod in patients with generalised myasthenia gravis (ADAPT): a multicentre, randomised, placebo-controlled, phase 3 trial. *Lancet Neurol*. 2021;20(7):526-536. doi:10.1016/S1474-4422(21)00159-9
10. Obaid AH, Zografou C, Vadysirisack DD, et al. Heterogeneity of acetylcholine receptor autoantibody–mediated complement activity in patients with myasthenia gravis. *Neurol Neuroimmunol Neuroinflamm*. 2022;9(4):e1169. doi:10.1212/NXI.0000000000001169
11. Khani-Habibabadi F, Roy B, Pham MC, et al. AChR autoantibody pathogenic properties are heterogeneously distributed and undergo temporal changes among patients with myasthenia gravis. *Neurol Neuroimmunol Neuroinflamm*. 2025;12(5):e200436. doi:10.1212/NXI.0000000000200436
12. Saxena A, Stevens J, Cetin H, et al. Characterization of an anti-fetal AChR monoclonal antibody isolated from a myasthenia gravis patient. *Sci Rep*. 2017;7(1):14426. doi:10.1038/S41598-017-14350-8
13. Ding S, Wu X, Li G, Han M, Zhuang Y, Xu T. Efficient transposition of the piggyBac (PB) transposon in mammalian cells and mice. *Cell*. 2005;122(3):473-483. doi:10.1016/j.cell.2005.07.013
14. Bayer AC, Sanmarco LM, Pellerin A, et al. Therapeutic IgG- and IgM-specific proteases disarm the acetylcholine receptor autoantibodies that drive myasthenia gravis pathology. *Proc Natl Acad Sci U S A*. 2025;122(43):e2505984122. doi:10.1073/PNAS.2505984122
15. Fuchs L, Shelly S, Vigiser I, et al. Real-world experience with efgartigimod in patients with myasthenia gravis. *J Neurol*. 2024;271(6):3462-3470. doi:10.1007/S00415-024-12293-5
16. Frangiamore R, Rinaldi E, Vanoli F, et al. Efgartigimod in generalized myasthenia gravis: a real-life experience at a national reference center. *Eur J Neurol*. 2024;31(4):e16189. doi:10.1111/ENE.16189
17. Losen M, Martínez-Martínez P, Phernambucq M, Schuurman J, Parren PWHI, De Baets MH. Treatment of myasthenia gravis by preventing acetylcholine receptor modulation. *Ann N Y Acad Sci*. 2008;1132(1):174-179. doi:10.1196/ANNALS.1405.034
18. Vincent A, Newsom-Davis J. Acetylcholine receptor antibody characteristics in myasthenia gravis. I. Patients with generalized myasthenia or disease restricted to ocular muscles. *Clin Exp Immunol*. 1982;49(2):257-265.
19. Lennon VA. Serologic profile of myasthenia gravis and distinction from the Lambert-Eaton myasthenic syndrome. *Neurology*. 1997;48(suppl_5):S23-S27. doi:10.1212/WNL.48.SUPPL_5.23S
20. Almon RR, Andrew CG, Appel SH. Serum globulin in myasthenia gravis: inhibition of α-bungarotoxin binding to acetylcholine receptors. *Science (1979)*. 1974;186(4158):55–57. doi:10.1126/SCIENCE.186.4158.55
21. Cetin H, Webster R, Liu WW, et al. Myasthenia gravis AChR antibodies inhibit function of rapsyn-clustered AChRs. *J Neurol Neurosurg Psychiatry*. 2020;91(5):526-532. doi:10.1136/JNNP-2019-322640
22. Meriggioli MN, Sanders DB. Muscle autoantibodies in myasthenia gravis: beyond diagnosis?. *Expert Rev Clin Immunol*. 2012;8(5):427-438. doi:10.1586/ECI.12.34
23. Novoselov AV, Rezaykin AV, Sergeev AG, Fadeyev FA, Grigoryeva JV, Sokolova ZI. A single amino acid substitution controls DAF-dependent phenotype of echovirus 11 in rhabdomyosarcoma cells. *Virus Res*. 2012;166(1-2):87-96. doi:10.1016/j.virusres.2012.03.007
24. Goodfellow IG, Powell RM, Ward T, Spiller OB, Almond JW, Evans DJ. Echovirus infection of rhabdomyosarcoma cells is inhibited by antiserum to the complement control protein CD59. *J Gen Virol*. 2000;81(5):1393-1401. doi:10.1099/0022-1317-81-5-1393
25. Yu J, Murthy V, Liu SL. Relating GPI-anchored Ly6 proteins uPAR and CD59 to viral infection. *Viruses*. 2019;11(11):1060. doi:10.3390/V11111060
26. Song C, Xu Z, Miao J, et al. Protective effect of ScFv-DAF fusion protein on the complement attack to acetylcholine receptor: a possible option for treatment of myasthenia gravis. *Muscle Nerve*. 2012;45(5):668-675. doi:10.1002/MUS.23247
27. Albazli K, Kaminski HJ, Howard JF. Complement Inhibitor therapy for myasthenia gravis. *Front Immunol*. 2020;11:917. doi:10.3389/fimmu.2020.00917
28. Mantegazza R, Salazar M, Mokhtari A, et al. The role of complement in the pathogenesis and treatment of myasthenia gravis. *Cells*. 2025;14(10):739. doi:10.3390/CELLS14100739
29. Falso S, Marini S, Morroni J, Marini M, Iorio R. Two paths for turning the tide: complement and FcRn inhibition to overcome refractory myasthenia gravis. *Neurol Sci*. 2025;46(12):7057-7060. doi:10.1007/S10072-025-08570-4